

In silico investigation of interactions between human cannabinoid receptor-1 and its antagonists

Guanglin Kuang · Guoping Hu · Xianqiang Sun ·
Weihua Li · Guixia Liu · Yun Tang

Received: 18 October 2011 / Accepted: 14 February 2012 / Published online: 9 March 2012
© Springer-Verlag 2012

Abstract Cannabinoid receptor-1 (CB₁) is widely expressed in the central nervous system and plays a vital role in regulating food intake and energy expenditure. CB₁ antagonists such as Rimonabant have been used in clinic to inhibit food intake, and therefore reduce body weight in obese animals and humans. To investigate the binding modes of CB₁ antagonists to the receptor, both receptor- and ligand-based methods were implemented in this study. At first, a pharmacophore model was generated based on 31 diverse CB₁ antagonists collected from literature. A test set validation and a simulated virtual screening evaluation were then performed to verify the reliability and discriminating ability of the pharmacophore. Meanwhile, the homology model of CB₁ receptor was constructed based on the crystal structure of human β_2 adrenergic receptor (β_2 -AR). Several classical antagonists were then docked into the optimized homology model with induced fit docking method. A hydrogen bond between the antagonists and Lys192 on the third transmembrane helix of the receptor was formed in the docking study, which has proven to be critical for receptor-ligand interaction by biological experiments. The structure obtained from induced fit docking was then confirmed to be a reliable model for molecular docking from the result of the simulated virtual screening. The consistency between the pharmacophore and the homology structure further proved the previous observation. The built receptor

structure and antagonists' pharmacophore should be useful for the understanding of inhibitory mechanism and development of novel CB₁ antagonists.

Keyword Cannabinoid receptor-1 · CB₁ antagonist · Homology modeling · Induced fit docking · Pharmacophore

Introduction

Endo-cannabinoid system consists of some endogenous ligands (such as anandamide, 2-arachidonoyl, *etc.*) and two cannabinoid receptor subtypes (CB₁ and CB₂). In regard to distribution and functionality, CB₁ receptor is predominantly expressed in the central nervous system and is probably responsible for most of the pharmacological effects of endo-cannabinoids, while CB₂ receptor is mainly found in peripheral tissues, such as spleen, tonsil, and immunocytes, and is involved in the signal transduction processes in the immune system [1–3]. Both subtypes belong to the class A family of G-protein-coupled receptor (GPCR), which is characterized by seven transmembrane α -helices connected by three extracellular loops (ECLs) and three intracellular loops (ICLs) [4, 5].

Obesity has become more and more prevalent nowadays and is gradually recognized as a serious health care problem which can result in hypertension and diabetes and thus needs special attention [6]. However, the approved drugs available to treat obesity are quite limited. Fenfluramine and dexfenfluramine, which were once first-line drugs to treat obesity, have been withdrawn due to potential of valvular heart diseases [7]. Therefore it is well worth the effort to develop novel and efficient anti-obesity agents with fewer side-effects. CB₁ receptor is of particular interest to us because of its regulation of appetite. The endo-cannabinoids play an important role,

Electronic supplementary material The online version of this article (doi:10.1007/s00894-012-1381-8) contains supplementary material, which is available to authorized users.

G. Kuang · G. Hu · X. Sun · W. Li · G. Liu · Y. Tang (✉)
Shanghai Key Laboratory of New Drug Design, School
of Pharmacy, East China University of Science and Technology,
130 Meilong Road,
Shanghai 200237, China
e-mail: ytang234@ecust.edu.cn

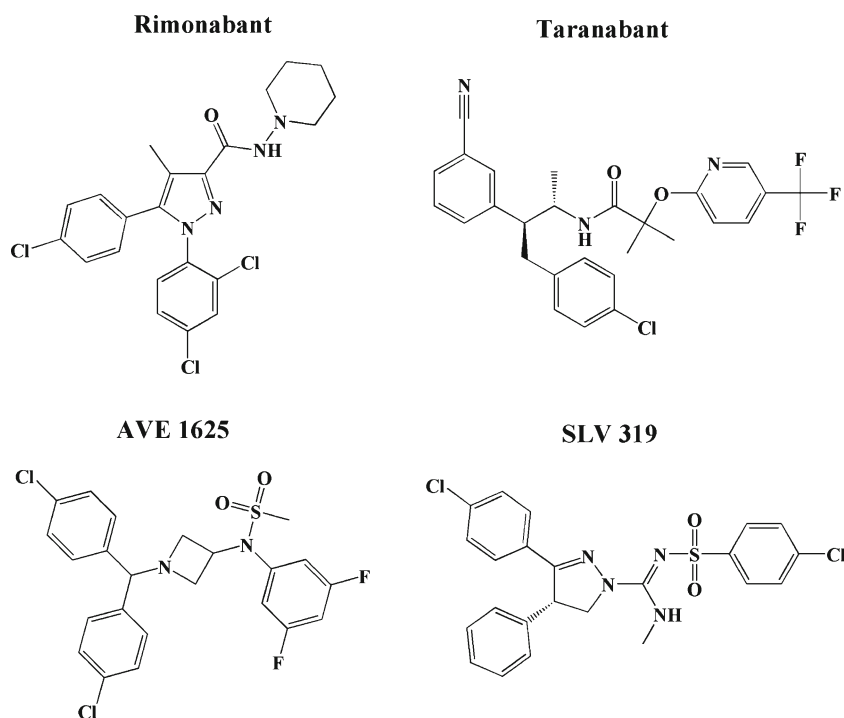
through CB₁ receptor, in regulating food intake and energy expenditure. CB₁ antagonists such as Rimonabant and Taranabant have proven to play an important role in inhibiting food intake and thus reduce body weight in obese animals and humans. Therefore, CB₁ antagonists are regarded as promising anti-obesity agents. Besides, it is reported that CB₁ antagonists can have good prospects in other therapeutic areas such as smoking, alcohol addiction and cognitive impairment [8, 9]. In the past two decades, a large number of synthetic CB₁ antagonists have been reported [10–26]. Rimonabant from Sanofi is the prototypical CB₁ antagonist and has been served as the template of many subsequent analogues. Moreover, this compound has entered the market in the European Union for treatment of obesity but was not approved by the U.S. Food and Drug Administration (FDA) due to concerns of influencing suicidal ideation [27]. Other analogues that have progressed into clinical trials include AVE 1625 from Aventis (Phase II), SLV 319 from Solvay/Bristol-Meyers Squibb (Phase III), and Taranabant (MK 0364) from Merck (Phase III), *etc.* (Fig. 1) [28].

In the past few years many computational methods have been employed in the investigation of CB₁ antagonists. For example, Shim *et al.* [29] developed a 3D-QSAR (CoMFA) model of CB₁ antagonists based on 28 molecules with the same pyrazole scaffold. Their model was properly constructed and could explain their experiment results. They also obtained some useful information for further lead optimization. However, it is generally believed that a single CoMFA model has quite limited application domain and is often just used to optimize lead compounds with the same scaffold [30]. Therefore, in this

study we chose a set of compounds which had broad activity range and diverse scaffolds in the hope that the reliability of the generated model could be guaranteed and the application domain be broadened. Besides, Wang *et al.* created a pharmacophore model based on eight CB₁ antagonists with Catalyst/HipHop module [10]. Their model was utilized for virtual screening and several novel ligands were identified successfully. However, pharmacophore models generated with HipHop were qualitative and thus could not explain the detailed structure-activity relationship of the ligands developed. In addition, their model was based merely on ligand information. Therefore, it would be useful to develop a quantitative pharmacophore model based on diverse CB₁ antagonists and meanwhile take receptor information into consideration.

Although the crystal structure of human CB₁ receptor has not been determined, homology modeling method can be used as a complementary method in structure prediction, especially in the field of GPCR. Many successful studies have been published in this research area [31–36]. Before human β_2 -adrenergic receptor (β_2 -AR) was determined in 2007 [37], the homology models of CB₁ receptor were based on the crystal structure of bovine rhodopsin [38–42]. Compared with bovine rhodopsin, β_2 -AR shares higher identity with CB₁. Therefore, we suppose that the results of homology modeling based on β_2 -AR would be more reliable. Recently, Shim *et al.* [43] built a homology model of the seven transmembrane α -helices of CB₁ receptor based on β_2 -AR, which is now regarded as the most reliable CB₁ model. However, extra- and intra-cellular loops also play an important role in GPCR [31, 32, 34], but no

Fig. 1 Structures of some typical CB₁ antagonists



attention was paid to these regions in Shim's study. Therefore, a receptor model with carefully handled loop regions is also a significant issue.

As we can see, previous research was accomplished with either receptor- or ligand-based method. We believe that the results would be more reliable and useful if receptor- and ligand-based methods are combined together. Therefore, in this work, ligand-based pharmacophore modeling, receptor-based homology modeling and molecular docking were implemented to investigate the critical chemical features and binding modes of CB₁ antagonists. These results can serve as useful information for the development of novel CB₁ antagonists as well as the understanding of inhibitory mechanism.

Materials and methods

Data set

Ninety-one representative CB₁ antagonists, whose activities were tested by the same biological protocol, were collected from literature [10–23, 27–29, 44]. Among them, 31 (Table 1) were selected as the training set for model generation according to scaffold diversity and the distribution of activities, and the remaining 60 compounds (Table S1) were used as the test set for model validation. The K_i values which spanned four orders of magnitude were used, instead of using the logarithmic values of them.

Table 1 Structures, experimental and predicted binding affinity (K_i) of training set molecules

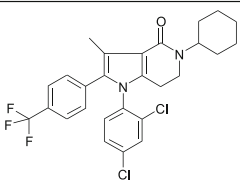
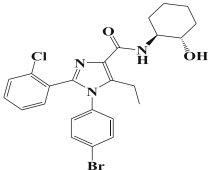
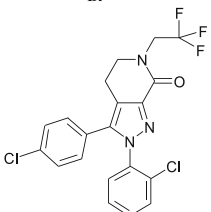
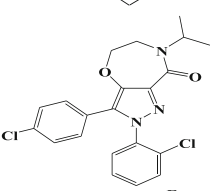
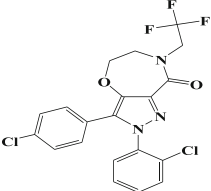
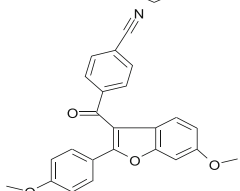
Compound No.	Structure	Experimental K _i (nM) ^a	Predicted K _i (nM)	Error ^b	Reference
Tr1		4.1	2.7	-1.5	[20]
Tr2		240	630	2.6	[20]
Tr3		1.7	1.5	-1.1	[23]
Tr4		1.3	2.2	1.7	[23]
Tr5		1.9	1.9	1.0	[23]
Tr6		141	350	2.4	[10]

Table 1 (continued)

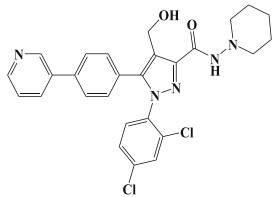
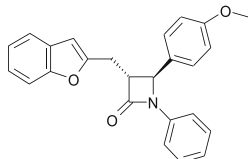
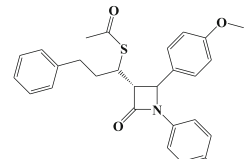
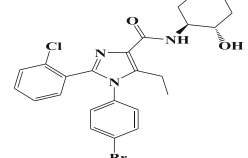
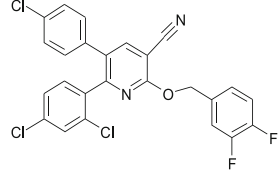
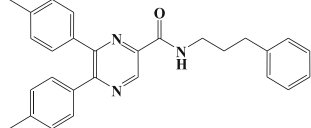
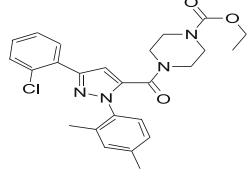
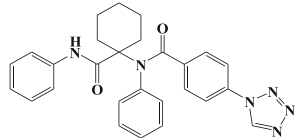
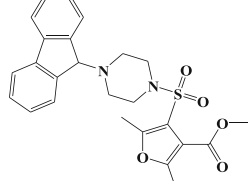
Compound No.	Structure	Experimental Ki (nM) ^a	Predicted Ki (nM)	Error ^b	Reference
Tr7		5.8	2.6	-2.3	[10]
Tr8		839	590	-1.4	[10]
Tr9		52.8	29	-1.8	[10]
Tr10		3.7	1.4	-2.6	[21]
Tr11		1.3	8.5	6.6	[21]
Tr12		18	23	1.3	[21]
Tr13		287	460	1.6	[19]
Tr14		1049	750	-1.4	[19]
Tr15		1606	1100	-1.4	[19]

Table 1 (continued)

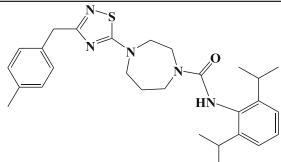
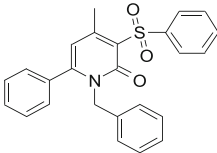
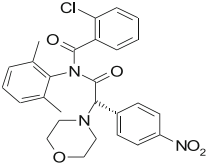
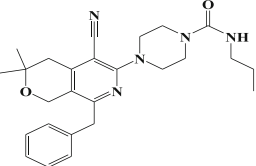
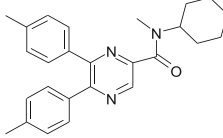
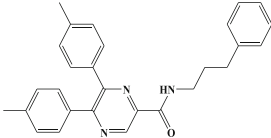
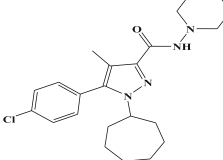
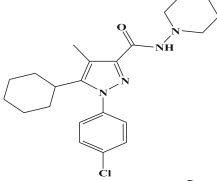
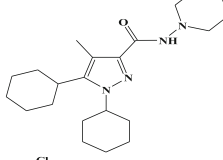
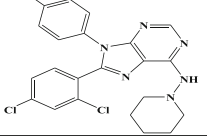
Compound No.	Structure	Experimental Ki (nM) ^a	Predicted Ki (nM)	Error ^b	Reference
Tr16		1764	370	-4.8	[19]
Tr17		2716	1600	-1.7	[19]
Tr18		2785	800	-3.5	[19]
Tr19		3949	2700	-1.5	[19]
Tr20		59	67	1.1	[18]
Tr21		18	23	1.3	[18]
Tr22		275	300	1.1	[12]
Tr23		318	350	1.1	[12]
Tr24		5110	23000	4.6	[12]
Tr25		7.4	15	2.0	[22]

Table 1 (continued)

Compound No.	Structure	Experimental K_i (nM) ^a	Predicted K_i (nM)	Error ^b	Reference
Tr26		7.1	15	2.1	[22]
Tr27		5.2	5.3	1.0	[22]
Tr28		38	110	3.0	[17]
Tr29		0.5	1.2	2.4	[17]
Tr30		1.0	1.2	1.2	[17]
Tr31		1.9	1.7	1.1	[17]

^a K_i values were all determined on human CB_1 receptor

^b The Error column shows the ratio of predicted activity to measured activity (or the ratio of measured activity to predicted activity, if that gives a number greater than 1, in which case the number is negative)

The 2D chemical structures of these compounds were sketched and then minimized with the CHARMM-like force field in Catalyst 4.10 [45]. The conformers of each compound were generated in Catalyst in the best quality mode. The maximal number of conformers was set to 250 with an energy threshold of 20 kcal/mol.

Generation and validation of pharmacophore models

In the absence of crystallographic data of CB_1 receptor, ligand-based pharmacophore modeling could serve as a complementary tool for the investigation of CB_1 antagonists. Catalyst is a

classical software for pharmacophore generation and has a set of methods to estimate and validate the results.

In this study, the pharmacophore models were constructed with the HypoGen module of Catalyst 4.10. When generating a hypothesis, Catalyst/HypoGen attempts to optimize the pharmacophore models based on the experimental values and the complexity of the hypothesis. The uncertainty value, which represents the uncertainty range of the measured biological activity for each compound, was set to 3 for compound activity. It can be deemed as a threshold of the experimental error. Analysis of the functional groups of each compound in the training set revealed that three types of chemical features,

namely hydrogen bond acceptor (HBA), hydrophobic group (HP), aromatic ring group (RA), were common to most training set molecules and thus were chosen as possible features for the pharmacophore generating process. The numbers of HBA, HP and RA were set to 1~5, 0~5 and 0~5, respectively and the minimum and maximum numbers of total features were set to 3 and 5, respectively. All the other parameters were set as default.

The best pharmacophore model was selected according to the comparison among the Catalyst parameters having specific statistical meanings. The selected pharmacophore model was then validated by test set prediction and simulated virtual screening test. 60 diverse CB₁ antagonists were used as a test set to verify the ability of the pharmacophore model to predict the binding affinity values of non-training set molecules.

The database used for subsequent simulated virtual screening test was composed of 30 actives and 1000 decoys. The actives were test set compounds whose IC₅₀ values were below 100 μM. The decoys were selected based on the protocols of Discovery Studio 2.1 [46]. Firstly, 258,512 molecules were retrieved from two common commercial compound database-Specs (<http://www.specs.net/>) and Maybridge (<http://www.maybridge.com/>). Secondly, with the “find diverse molecules” protocol, 10,000 diverse compounds were chosen from the 258,512 molecules. Finally, with the “find similar molecules by fingerprint” protocol, 1000 similar compounds were obtained from these 10,000 diverse molecules using the 30 known CB₁ antagonists as references. During this process, similarity calculation was first performed between the 10,000 diverse molecules and the 30 actives based on FCFP₄ fingerprint, and then the top 1000 molecules sorted by the Tanimoto similarity index values were collected as the decoy set. These three consecutive steps not only ensured the structural diversity of selected decoys but also kept them localized near the chemical space of the active molecules. This process has been confirmed to be reliable by a previous study of our group [47]. Subsequently, the database was screened with the “ligand pharmacophore mapping” protocol in the “best flexible search” and “fast conformation generation” pattern of Discovery Studio 2.1.

Homology modeling

The primary sequence of human CB₁ receptor (Accession ID: P21554) containing 472 amino acids was downloaded from the Swiss-Prot website (<http://www.expasy.ch/sprot/>) [48]. The crystal structure of human β₂-adrenergic receptor (PDB ID: 2RH1) was obtained from the Protein Data Bank website (<http://www.rcsb.org/pdb/>) [49]. The crystal structure of 2RH1 was prepared with the protein preparation workflow in Maestro 8.5 [50] before it was used as the template for

homology modeling. During this process, water molecules were deleted, hydrogen atoms were added and problematic side chains were fixed. The T4-lysozyme, which was used to stabilize the structure in the crystallizing process, was deleted from the 2RH1 structure. The original ligand of 2RH1-Carazol was kept, so that the homology model would have a ligand in the same region.

The sequence alignment between P21554 and 2RH1 was accomplished using Prime 2.0 module [51]. Some residues were manually aligned to make sure that there were no gaps in the helix regions and most of conserved residues could be aligned. The sequence identity of the final sequence alignment was 29%. Based on this alignment, a homology model was built. This model was then submitted to loop and side chain refinement jobs. The resulting model was finally minimized using MacroModel 9.6 [52] with the OPLS₂₀₀₀ all-atom force field.

The quality of the homology model was checked with the Procheck program [53]. A Ramachandran plot was generated by Procheck with a resolution of 2.4 angstroms (Å), which was the resolution of 2RH1. The final homology model was aligned with the prepared structure of 2RH1 with the proteins aligning module in Maestro 8.5.

Molecular docking and simulated virtual screening

In this work, several classical CB₁ antagonists were selected for docking study. The induced fit docking (IFD) workflow of Maestro 8.5 was utilized to dock the antagonists into the homology model of CB₁ receptor. Before docking, the antagonists were prepared with the LigPrep [54] module of Maestro 8.5. LigPrep was used to generate low-energy 3D structures of the antagonists which would serve as the input ligand structures in the subsequent docking studies.

The IFD workflow utilized Prime 2.0 [51] and Glide 5.0 [55] to induce adjustments in the receptor structure, especially within the binding pocket. This workflow set up a sequence of jobs where ligands were first docked into the receptor with Glide, then Prime refinement was implemented to allow the receptor to relax, and finally the ligands were redocked into the relaxed receptor with Glide again. The adjustment and docking processes were all accomplished automatically and successively. The grid-enclosing box was centered on Lys 192 and the box size was set to Auto and thus was 10 Å on each side. All the other parameters were left as default.

To evaluate the effect of induced fit docking, a simulated virtual screening test was carried out. The receptor structures were the homology models of CB₁ receptor before and after the induced fit docking process. Glide 5.0 was used to generate the grid files of the homology models with the original ligands as the grid centers. Then Glide standard

precision (SP) was employed to dock database compounds into the grid files. The results of these two models could then be compared.

Building of consensus model

The pharmacophore model of CB₁ antagonists and the homology model of CB₁ receptor were generated from the information of ligands and receptor, respectively. They should be able to validate the reliability of each other. In this study, we combined these two models together, namely to map the pharmacophore model with the homology model. If the chemical features of the pharmacophore model could map with the critical residues of the homology model properly, then the consistency of these two models was achieved. We could call this kind of combined model a consensus model. This process was accomplished with Discovery Studio 2.1 and Maestro 8.5. Firstly, CB₁ antagonists were mapped with the pharmacophore in the flexible and best patterns with the “ligand pharmacophore mapping” protocol. Secondly, based on the results of IFD docking, the poses of CB₁ antagonists having appropriate binding modes and docking scores were obtained from Maestro. Finally, the pharmacophore aligned with the antagonists was superimposed onto the aforementioned poses. The characteristics of the combined model were then analyzed visually to check whether a consensus model could be obtained.

Results and discussion

Pharmacophore generation and validation

Thirty-one compounds (Table 1) which were diverse both in structure and activity were used as training set to generate pharmacophore models. Ten models were generated in all based upon the settings described in the Materials and methods section. Table 2 shows the ten hypotheses as well as some important parameters such as Δ cost, correlation, configuration, etc., which were generated by Catalyst automatically.

As a rule, if the configuration value is less than 18, a thorough analysis of all models is carried out. If higher, Catalyst will truncate the list and some models would not be considered, so the results might be incomplete. In our study, the configuration value is 14.1 and thus is acceptable.

Fixed cost is the cost of an ideal model which fits all data perfectly while null cost is the cost of a null model which has no features at all and whose estimated activity is the average of the activity values of training set molecules. These two models represent the upper and lower limits for the generated models. During an automated pharmacophore generating process, Catalyst calculates and discards many thousands of models. The overall assumption is based on Occam's razor [56] which believes that among all the equivalent alternatives, the simplest

Table 2 Results of the top ten pharmacophore hypotheses generated from the training set with the Catalyst/HypoGen module

Hypothesis no.	Features	Total cost	Δ cost	RMSD
1	AHRR	134.2	86.9	0.827
2	AHRR	137.3	84.1	0.940
3	AHRR	137.3	84.1	0.945
4	AHRR	138.5	82.6	0.986
5	AHRR	138.8	82.3	0.999
6	AHRR	139.5	81.6	1.02
7	AHRR	140.0	81.1	1.03
8	AHRR	140.1	81.0	1.04
9	AHRR	140.4	80.7	1.05
10	AHRR	140.9	80.2	1.05

A: hydrogen bond acceptor; H: hydrophobic group; R: ring aromatic group

Fixed cost=122.8; Null Cost=221.1; Δ cost=Null cost-Total cost

model is the best one. In this case the model whose cost value is closest to the fixed cost is the best one. Thus in terms of hypothesis significance, what really matters is the magnitude of the difference between the cost of any returned model and the cost of the null model. In general, if the difference is greater than 60, there is an excellent chance (>90%) that the model represents a true correlation. If the difference ranges from 40 to 60, there is a 75-90% chance of representing the true correlation of the data [45]. In this research, the fixed cost and null cost of the pharmacophore generating process were 122.8 and 221.1, respectively. The difference between the fixed cost and null cost was 98.3, which meant that the training set molecules plus the Catalyst settings were likely to produce reliable models. As a matter of fact, the Δ cost values of the top ten pharmacophore models ranged from 80.2 to 86.9 (Table 2). Therefore, all those models were reasonable in terms of Δ cost values.

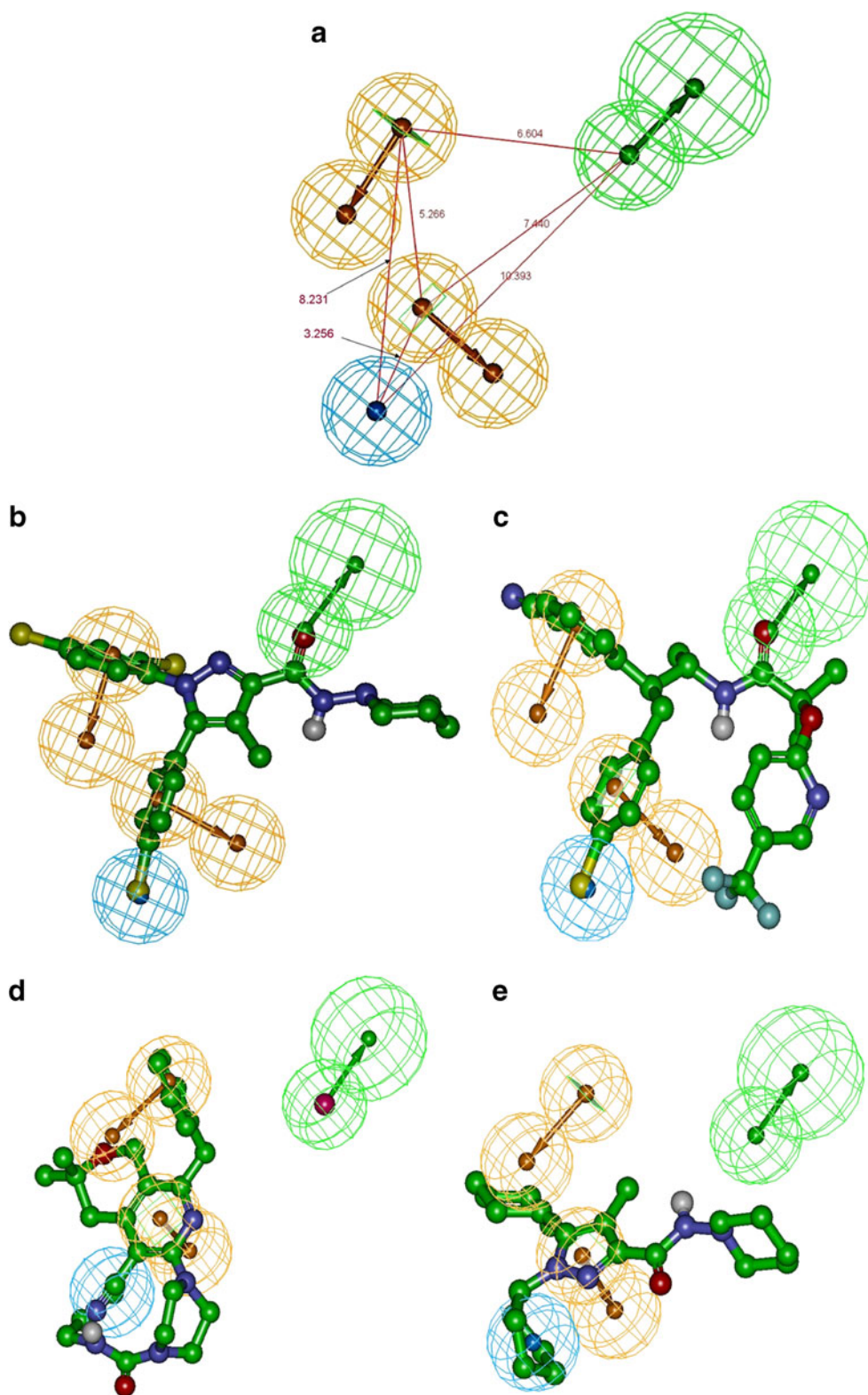
Hypo 1 showed optimal values of all kinds of parameters, such as Δ cost, root mean square deviation (RMSD) and correlation, etc. The total cost of Hypo 1 was 134.2 which was closest to the fixed cost and at the same time furthest from the null cost. Therefore, Hypo 1 was the best model among the top ten according to Occam's assumption. The Δ cost of Hypo 1 was 86.9 and thus the probability that Hypo 1 could represent a true correlation of the data was greater than 90%. The RMSD factor represents the deviation of the log(estimated activities) from the log(measured activities) normalized by the log(uncertainties). This parameter indicates the quality of prediction for training set and the smaller is the better. The RMSD value of Hypo 1 was 0.827 which was the smallest and therefore the best. The correlation coefficient of training set molecules is another important indicator of the quality of the models. Like RMSD value, correlation coefficient of the training set can also indicate the predictive ability of a model. The

correlation coefficient of Hypo 1 was 0.951 and was the largest one. Therefore Hypo 1 could be deemed as the best pharmacophore model according to the analysis of above statistical parameters.

Fig. 2 Pharmacophore model of CB₁ antagonist generated with Catalyst/HypoGen. (a): Geometrical relationship among pharmacophore features.

Aromatic ring groups (RA) are represented by two pairs of brown meshed spheres, hydrophobic group (HP) by a cyan sphere and hydrogen bond acceptor (HA) by a pair of green spheres where the smaller one represents the location of the hydrogen bond acceptor atom on the ligand and the larger one the location of a hydrogen bond donor atom on the receptor. The distances (Å) among the centers of the features are labeled. (b), (c), (d) and (e) are the mapping patterns of Rimonabant, Tarabanant, Tr19 and Tr24 to the pharmacophore, respectively. Carbon atoms are colored in green, nitrogen atoms in blue, oxygen atoms in red, chlorine atoms in light yellow, fluorine atoms in cyan and hydrogen atoms in gray. Non-polar hydrogen atoms are not shown for clarity

Hypo 1 is illustrated in Fig. 2a. The distances between every two features are also displayed. Figures 2b and 2c show the mapping of two highly potent (K_i <10 nM) CB₁ antagonists with Hypo 1. The first one is Rimonabant with a



classic pyrazole core and the second one is Taranabant which is acyclic. It can be seen that all the features of Rimonabant and Taranabant can fit the pharmacophore quite well. The structures of Rimonabant and Taranabant are significantly distinct from each other (Fig. 1), yet both are quite active. What's more, Rimonabant belongs to the training set while Taranabant does not. This proves that the pharmacophore we generated has a relatively broad application domain. Figures 2d and 2e demonstrate the mapping of Hypo 1 with two compounds having low potency ($K_i > 1000$ nM). As we can see, the mapping patterns of them are much worse than those of Rimonabant and Taranabant. Comparison of the mapping patterns of the pharmacophore with these four compounds reveals that the hydrogen bond acceptor features of D and E cannot be mapped while the hydrophobic group and aromatic ring features can be mapped to some extent. Therefore, it indicates that the hydrogen bond acceptor feature should be critical for a compound to be an active CB_1 antagonist.

The predictive ability of the pharmacophore was first validated with a test set of 60 CB_1 antagonists which had diverse structures and a wide range of activity values (Table S1). The test set compounds were prepared with the same method as that of the training set molecules. The correlation coefficient of the test set is 0.81 (Fig. 3) and thus suggests a good correlation between the measured and estimated binding affinities of test set compounds.

The simulated virtual screening was aimed to evaluate the discriminating ability of the pharmacophore to tell active CB_1 antagonists from inactive ones. The evaluation of the performance of simulated virtual screening is an important but error-prone process. Enrichment factor (EF) evaluates the improvement of hit rate by a virtual screening method versus random selection at different screening stages (e.g.,

5% or 10%). However, it has been criticized for its shortcoming of high dependency on the ratio of actives and decoys in the database [57]. Alternatively, in this study we used ROC enrichment factor (ROCEF), which was defined as the ratio of true positive rate to false positive rate at a given stage where certain specific percentage of the decoys had been observed. This measurement was similar to EF but did not show a high dependency on the actives/decoys ratio [58]. Additionally, we also reported an overall measurement called area under the curve (AUC) for virtual screening against the whole data set. As with EF, ROCEF over 1.0 indicates that the enrichment is better than random selection at certain decoy stages, and an AUC value approaching 1.0 signifies an ideal discrimination of actives from decoys. The ROC curve of the simulated virtual screening of the pharmacophore is presented in Fig. 4. In this study, the AUC value is 0.781 and thus is much better than random selection. Besides, the ROC enrichment factor at 10% decoy stage is 7.6. This means that the enrichment is 7.6 folds higher for virtual screening than random selection at this stage.

There was a similar study reported by Telvekar et al. [59] recently. They generated a pharmacophore model based on a series of 1-sulfonyl-4-acylpiperazine derivatives with phase of Maestro, Schrödinger [50]. Their pharmacophore model consisted of one hydrogen bond acceptor, two hydrophobic groups and two aromatic rings. This model had one more hydrophobic group than ours. According to our observations in this study, those two aromatic groups would take part in some critical π - π aromatic interactions in the ligand-receptor binding modes. However, the hydrophobic interaction did not show such important function. This additional hydrophobic feature might make the model too restricted. Based on the alignment of training set molecules, they

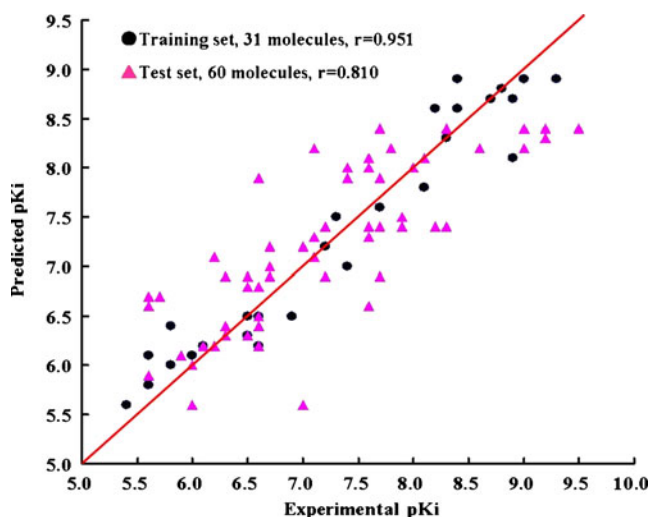


Fig. 3 Graph showing the correlation between measured and predicted binding affinity (pK_i) values of the training set and test set molecules

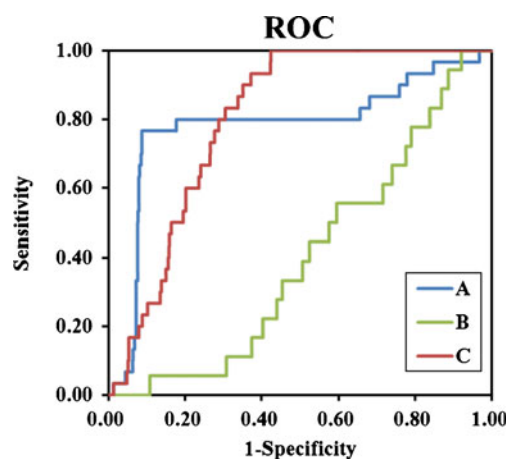


Fig. 4 ROC curves of the simulated virtual screening tests of pharmacophore mapping (a) and molecular docking (b, homology model before induced fit docking; c, homology model after induced fit docking)

conducted 3D-QSAR studies with CoMFA and CoMSIA of Sybyl, Tripos, in an effort to validate the robustness of the pharmacophore model. Compared with the results of Telvekar et al. model, our pharmacophore was improved in two aspects. Firstly, our training set had broader diversity, which covered a range of scaffolds whereas theirs was based on 1-sulfonyl-4-acylpiperazine derivatives. Secondly, as a whole, the predictive ability of our model had been improved. The correlation coefficients of the training set and test set in our study were higher than the counterparts of theirs.

Another similar study was reported by Weber et al., who performed 2D and 3D QSAR investigations based on a series of diarylpyridines which acted as CB₁ ligands by means of hologram quantitative structure–activity relationship (HQSAR) and CoMFA methods [60]. The HQSAR method in their study was rather innovative and could have significant implications. Both of their models had good statistical results, as well as internal and external consistency. With the development of medicinal chemistry, more CB₁ antagonists had been synthesized when our model was generated. Therefore we could use more novel compounds in the test set, which would make the results more reliable and convincing. Besides, an additional simulated virtual screening test was also implemented in our study and gave good results, which proved that the discriminative capability of our model was also satisfactory. To further validate the pharmacophore model generated in this study, we used the model to predict the activities of the test set compounds of Weber et al. The results were presented in Fig. S4 and Table S2. Overall, the predicting performance of our model was acceptable. The r^2 value of our model was 0.76 which was comparable to that of HQSAR method (0.80) but better than that of the CoMFA model (0.52). Besides, the two-dimensional contribution maps and 3D contour maps in their study were also in good agreement with the critical pharmacophore features in our study. For instance, the electrostatic field contour in their study corresponds to the hydrogen bond acceptor feature of our model and the nearby green bulk group corresponds to one of the aromatic ring groups of our model. The r^2 values of test set compounds and the consistence of chemical features further proved the validity of our model.

Construction and validation of homology model

Figure 5 shows the sequence alignment of human CB₁ receptor and human β_2 -adrenergic receptor (β_2 -AR). As we can see, most of the conserved residues reported by Baldwin et al. [61] are finely aligned. Based on this alignment, a homology model of CB₁ receptor was constructed (Fig. S1). After refinement and minimization, the homology model was aligned with the template structure 2RH1. The RMSD value between them was 1.20 which indicated that the model generated was acceptable and no manifest deviation was observed. The optimized model was then examined by the Procheck program which gave a

Ramachandran plot (Fig. S2). The result was rather satisfactory: 92.9% of the residues lay in the most favored regions, 6.0% in the additional allowed regions, 1.2% in the generously allowed regions and none in the disallowed regions.

During a classical molecular docking process, the receptor is held rigid while the ligand is free to change conformation. However, the assumption of a rigid receptor can often give misleading results, because in reality most proteins would undergo significant side-chain or backbone movements upon ligand binding. These changes allow the receptor to alter its binding site so that it can conform more closely to the shape of the ligand. This process is often referred to as “induced fit” and is one of the main tricky problems in structure-based drug design.

Some classical and highly potent CB₁ antagonists were docked into the ligand binding site of the homology model by the induced fit docking (IFD) workflow of Maestro 8.5. The docking result of Rimonabant shows that a hydrogen bond is formed between the carbonyl group and Lys192 (TMH3) (Fig. 6a). This kind of hydrogen bond interaction was also observed for other antagonists (Fig. S3). According to previous experimental studies, especially the mutation research, Lys192 in the third transmembrane helix was believed to play a critical role in the ligand-receptor binding interaction [24–26]. Besides the hydrogen bond interaction, Rimonabant also forms hydrophobic interaction with several residues, such as Phe174, Phe178, Phe200, Phe278, Trp279, Trp356, and Phe379. This observation is also consistent with previous experimental studies [62]. The hydrophobic interaction, most of which is aromatic π - π stacking interaction, though not as specific as hydrogen bond interaction, is also important for ligand binding.

To further evaluate the validity of the homology model of CB₁ receptor, a simulated virtual screening test with Glide standard precision (SP) [55] was implemented. The homology models (model 1 and model 2) before and after induced fit docking were used as the receptor structure, respectively. The results of both models are presented in Fig. 4. As we can see, the result of model 2 is much better than that of model 1. The AUC value of model 1 is 0.40 which is even lower than that of random selection (0.50). This is due to the fact that the binding pocket of model 1 was not optimized and thus might have some steric collision with the ligands and this would in turn give misleading results. By comparison, the result of model 2 is much better and its AUC value (0.80) is comparable with that of the pharmacophore (0.78). This indicates that induced fit docking of the homology model with active ligands is able to optimize the binding pocket and make it similar to its realistic state. The high AUC value of model 2 suggests that the homology model after induced fit docking is suitable to be used as the receptor structure in molecular docking.

Before the crystal structure of β_2 -AR was determined in 2008, reported homology models of CB₁ receptor were

Fig. 5 Sequence alignment of CB₁ receptor with β_2 -adrenergic receptor. Marked are conserved residues and particularly those in red are identical ones

Receptor	Sequence	End residue
	N-TERM TMH1 ICL1	
CB ₁ R	NFMDIECFMVLNPSQQLAIAVLSLTIGTFTVLENLVLVCLHRSRLRCR	150
β_2 AR	~~~~~DEVVVVGMGI VMSLIVLAI VFGNVLVITAAKFERLQT~	66
	TMH2 ECL1	
CB ₁ R	PSYHFVIGSLAVADLLGSVIFVYSFIDFHFV~HRKDSRNVFLKLGQVTS	199
β_2 AR	VTNYFITSLACADLVMLAVV PFGAAHILMKMWTFGNFWCEFWTSIDVLC	116
	TMH3 ICL2 TMH4	
CB ₁ R	FTASVGSIFLTAIDRYISIHRELAIKRIVTRPKAVVAFCLMWTIAIVIAV	249
β_2 AR	VTASIEITLCVIAVDRYFAITSDFKYQSLITKNKARVILMLWIVSGLTSF	166
	ECL2 TMH5	
CB ₁ R	LPILG~~~~~WNCEKLSVCSDIIPHIDETYLMEFWIGVTSVLLLFIV	291
β_2 AR	LPVQMHWYRATHQEA INCYAETCCDEFITNOAYA LASSIVSFYVPLVIMV	216
	ICL3	
CB ₁ R	YAYMYLLWKAHSHAVRMIQRGTQKSI I IHTSEDKGVQVTRPDQARMIRL	341
β_2 AR	FVYSRVFQEA KRQ~~~~~LKFCLKEHKA	271
	TMH6 ECL3 TMH7	
CB ₁ R	AKTIVLII VVLIICWGPLLAIMVYD VFGKMKLIKT VFAFCSMLCLINST	391
β_2 AR	LKTLGIIMGFTLCWLEFFIIVNI VHI~QDNLIRKEVYIILLNWIGVYNSG	320
	C-TERM	
CB ₁ R	VNPIIYALRSKDLRHAERSMFPSCEGTAQPLD NSMGDSDCLHKHANNAAS	441
β_2 AR	FNPLIYC~RSPDFRIAPQELLC L~~~~~	342

constructed on the basis of the crystal structure of bovine rhodopsin [38–40]. The sequence identities β_2 -AR and bovine rhodopsin with human CB₁ receptor are 29% and 25%, respectively. It is believed that a high sequence identity is essential for a reliable homology model. Therefore our model is supposed to be more reasonable than previous ones on this aspect. For example, in the homology model constructed by Shim et al. [38], several CB₁ ligands such as CP47497 and CP55940 were docked into the model and found that a key hydrogen bond was formed between Lys192 and the ligands, which was consistent with our results. In another model developed by Salo et al. [39], similar role of residue Lys192 was proposed for the potency of CB₁ ligands.

They also suggested that several aromatic residues such as Phe200, Tyr275 and Trp356 would take part in π - π stacking interactions with the ligands, which was in good agreement with our findings as illustrated in Fig. 6.

The models based on β_2 -AR are relatively scarce. Shim et al. reported a CB₁ receptor model based on β_2 -AR [43]. Their model shed light on some critical interactions among transmembrane helices. However, it did not take the intracellular and extracellular loops into consideration, which were believed to play an important role in the ligand-receptor binding interaction as well. What's more, they also helped to form the binding pocket CB₁ receptor. Therefore, the model built in this study is supposed to be more reasonable for the

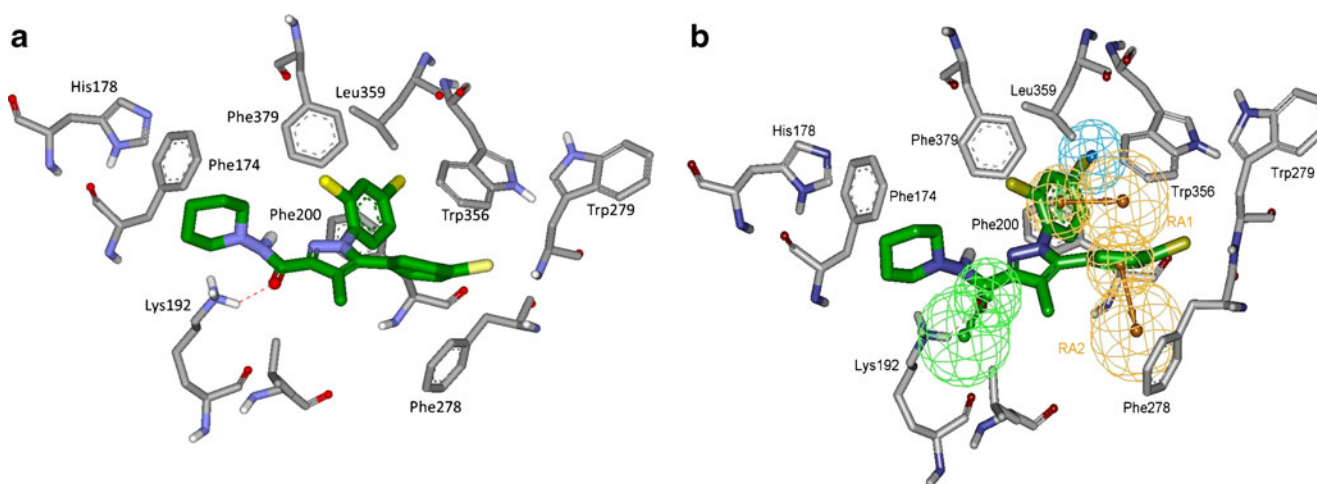


Fig. 6 (a) Detailed interaction of Rimobant with the homology model of CB₁ receptor. (b) Consensus model generated by mapping of the pharmacophore model to the binding site of the CB₁ homology model. Rimobant and amino acids are displayed in stick mode. The carbons of

the ligand are shown in green while those of the amino acids in gray. The hydrogen bond is presented as red dash lines. Only polar hydrogens are displayed for clarity

studying of ligand-receptor binding interaction as well as receptor-based drug design.

Consensus model

The consensus model was created with CB₁ antagonists as the common ligands in both the pharmacophore model (hypo 1) and the receptor homology model (model 2) as demonstrated in the Materials and methods section. Figure 6b shows the consensus model with Rimonabant as the common ligand. It can be seen that the hydrogen bond acceptor feature overlaps with the terminal amine of Lys192, which indicates that the ligand would form a hydrogen bond with the receptor in this region. Besides, the aromatic ring feature RA1 is almost parallel with the phenyl rings of Phe200 and Phe379 and the indole ring of Trp356. Another aromatic ring feature RA2 is approximately parallel with the phenyl ring of Phe278, though not so perfect as RA1. The mapping of the aromatic ring features with relevant aromatic residues indicates that Rimonabant can have manifest π - π stacking interactions with Phe200, Phe278, Trp256 and Trp379. Last but not least, the hydrophobic feature is located in the hydrophobic domain around Leu356, Trp359, etc. and thus can have hydrophobic interaction with these residues. All this information shows that our pharmacophore model generated based on the ligands alone is in good agreement with the docking results considering both the receptor and the ligand. This consistency is able to testify the rationality of both models. It can also identify some important features of the receptor-ligand interaction mode. In this study, the hydrogen bond acceptor and aromatic ring features were found to be critical for both models. Therefore, in further studies such as virtual screening and lead optimization, we should pay special attention to these features.

It should be noted that the mapping of the predocked ligand to the pharmacophore is not as perfect as that shown in Fig. 2b, where the information of the receptor is not considered. One possible explanation is that the ligand conformation mapping best with the pharmacophore is not the same as that interacting most favorably with the receptor. But the difference is acceptable and thus the results can still provide useful information for the development and optimization of CB₁ antagonists.

Generally speaking, pharmacophore mapping is much faster than molecular docking—in this case it is ten times faster, but the efficiency may not be so good [63]. For large databases such as Enamine which have millions of compounds, molecular docking would be very time-consuming. The consensus of the pharmacophore model and homology model developed in this study proved the reliability of each other mutually. Therefore they can be used together in further studies. The most important utility of them is to be implemented together in the so-called combined strategy of virtual screening, where pharmacophore mapping is first used to filter the compounds

which do not have essential features and then molecular docking is employed to choose those having excellent docking scores and specific binding modes. In this way, the speed can be increased several times yet the result would still be similar or even better. The combined strategy of pharmacophore mapping and molecular docking can thus increase speed and efficiency simultaneously.

Conclusions

In this study, CB₁ pharmacophore models were generated based on 31 diverse antagonists. The best model consisted of four features, namely one hydrogen bond acceptor, one hydrophobic center and two aromatic rings. This model had a high Δ cost value of 86.9, which indicated that the reliability of this model would be more than 90%. The correlation coefficients between experimental and predicted K_i values were 0.95 and 0.81 for the training set and test set, respectively. Meanwhile, a homology model of human CB₁ receptor was built based on the crystal structure of human β_2 -adrenergic receptor. Residue Lys192 in the third transmembrane helix of CB₁ receptor was found to form a critical hydrogen bond with antagonists. In addition, residues Phe174, Phe178, Phe200, Phe278, Trp279, Trp356, and Phe379 could form π - π stacking and hydrophobic interactions with those antagonists. These observations were consistent with previously experimental results. The homology model after induced fit docking proved to be suitable to be used as receptor structure in molecular docking, the result of which was even better than that of pharmacophore mapping. Finally, a consensus model was generated by combining the pharmacophore model and homology model together. The pharmacophore features of CB₁ antagonists and the key residues of the receptor could map pretty well. The consistency of them could validate each other mutually. These findings might be helpful for the understanding of inhibitory mechanism as well as the development and optimization of CB₁ antagonists.

Acknowledgments This work was supported by the Program for New Century Excellent Talents in University (Grant NCET-08-0774), the 863 High-Tech Project (Grant 2006AA020404), the 111 Project (Grant B07023), and the Shanghai Committee of Science and Technology (Grant 11DZ2260600).

References

1. Hanus L, Abu-Lafi S, Frider E, Breuer A, Vogel Z, Shalev DE, Kustanovich I, Mechoulam R (2001) 2-arachidonoyl glyceryl ether, an endogenous agonist of the cannabinoid CB1 receptor. *Proc Natl Acad Sci U S A* 98(7):3662–3665. doi:10.1073/pnas.061029898
2. Howlett AC, Barth F, Bonner TI, Cabral G, Casellas P, Devane WA, Felder CC, Herkenham M, Mackie K, Martin BR, Mechoulam R, Pertwee RG (2002) International Union of Pharmacology. XXVII.

- Classification of cannabinoid receptors. *Pharmacol Rev* 54(2):161–202
3. Boyd ST (2006) The endocannabinoid system. *Pharmacotherapy* 26(12 Pt 2):218S–221S. doi:10.1592/phco.26.12part2.218S
 4. Matsuda LA, Lolait SJ, Brownstein MJ, Young AC, Bonner TI (1990) Structure of a cannabinoid receptor and functional expression of the cloned cDNA. *Nature* 346(6284):561–564. doi:10.1038/346561a0
 5. Lu ZL, Saldanha JW, Hulme EC (2002) Seven-transmembrane receptors: crystals clarify. *Trends Pharmacol Sci* 23(3):140–146
 6. James PT, Leach R, Kalamara E, Shayeghi M (2001) The worldwide obesity epidemic. *Obes Res* 9:228S–233S
 7. Connolly HM, Crary JL, McGoon MD, Hensrud DD, Edwards BS, Edwards WD, Schaff HV (1997) Valvular heart disease associated with fenfluramine-phentermine. *N Engl J Med* 337(9):581–588
 8. Woods SC (2007) Role of the endocannabinoid system in regulating cardiovascular and metabolic risk factors. *Am J Med* 120(3 Suppl 1):S19–S25. doi:10.1016/j.amjmed.2007.01.004
 9. Carai MA, Colombo G, Gessa GL (2005) Rimonabant: the first therapeutically relevant cannabinoid antagonist. *Life Sci* 77(19):2339–2350. doi:10.1016/j.lfs.2005.04.017
 10. Wang HW, Duffy RA, Boykow GC, Chackalamannil S, Madison VS (2008) Identification of novel cannabinoid CB1 receptor antagonists by using virtual screening with a pharmacophore model. *J Med Chem* 51(8):2439–2446. doi:10.1021/Jm701519h
 11. Murineddu G, Ruiu S, Loriga G, Manca I, Lazzari P, Reali R, Pani L, Toma L, Pinna GA (2005) Tricyclic pyrazoles. 3. Synthesis, biological evaluation, and molecular modeling of analogues of the cannabinoid antagonist 8-chloro-1-(2',4'-dichlorophenyl)-N-piperidin-1-yl-1,4,5,6-tetrahydrobenzo [6, 7]cyclohepta[1,2-c]pyrazole-3-carboxamide. *J Med Chem* 48(23):7351–7362. doi:10.1021/jm050317f
 12. Krishnamurthy M, Li W, Moore BM (2004) Synthesis, biological evaluation, and structural studies on N1 and C5 substituted cycloalkyl analogues of the pyrazole class of CB1 and CB2 ligands. *Bioorg Med Chem* 12(2):393–404. doi:10.1016/j.bmc.2003.10.045
 13. Katoch-Rouse R, Pavlova OA, Caulder T, Hoffman AF, Mukhin AG, Horti AG (2003) Synthesis, structure-activity relationship, and evaluation of SR141716 analogues: Development of central cannabinoid receptor ligands with lower lipophilicity. *J Med Chem* 46(4):642–645. doi:10.1021/Jm020157x
 14. Shu H, Izenwasser S, Wade D, Stevens ED, Trudell ML (2009) Synthesis and CB1 cannabinoid receptor affinity of 4-alkoxycarbonyl-1,5-diaryl-1,2,3-triazoles. *Bioorg Med Chem Lett* 19(3):891–893. doi:10.1016/j.bmcl.2008.11.110
 15. Muccioli GG, Martin D, Scriba GKE, Poppitz W, Poupaert JH, Wouters J, Lambert DM (2005) Substituted 5,5'-diphenyl-2-thioxoimidazolidin-4-one as CB1 cannabinoid receptor ligands: Synthesis and pharmacological evaluation. *J Med Chem* 48(7):2509–2517. doi:10.1021/Jm049263k
 16. Lan RX, Liu Q, Fan PS, Lin SY, Fernando SR, McCallion D, Pertwee R, Makriyannis A (1999) Structure-activity relationships of pyrazole derivatives as cannabinoid receptor antagonists. *J Med Chem* 42(4):769–776
 17. Carpino PA, Griffith DA, Sakya S, Dow RL, Black SC, Hadcock JR, Iredale PA, Scott DO, Fichtner MW, Rose CR, Day R, Dibrino J, Butler M, DeBartolo DB, Dutcher D, Gautreau D, Lizano JS, O'Connor RE, Sands MA, Kelly-Sullivan D, Ward KM (2006) New bicyclic cannabinoid receptor-1 (CB1-R) antagonists. *Bioorg Med Chem Lett* 16(3):731–736. doi:10.1016/j.bmcl.2005.10.019
 18. Ellsworth BA, Wang Y, Zhu YH, Pendri A, Gerritz SW, Sun C, Carlson KE, Kang LY, Baska RA, Yang YF, Huang Q, Burford NT, Cullen MJ, Johngar S, Behnia K, Pelleymounter MA, Washburn WN, Ewing WR (2007) Discovery of pyrazine carboxamide CB1 antagonists: The introduction of a hydroxyl group improves the pharmaceutical properties and in vivo efficacy of the series. *Bioorg Med Chem Lett* 17(14):3978–3982. doi:10.1016/j.bmcl.2007.04.087
 19. Foloppe N, Benwell K, Brooks TD, Kennett G, Knight AR, Misra A, Monck NJT (2009) Discovery and functional evaluation of diverse novel human CB1 receptor ligands. *Bioorg Med Chem Lett* 19(15):4183–4190. doi:10.1016/j.bmcl.2009.05.114
 20. Smith RA, Fathi Z, Brown SE, Choi S, Fan J, Jenkins S, Kluender HC, Konkar A, Lavoie R, Mays R, Natoli J, O'Connor SJ, Ortiz AA, Podlogar B, Taing C, Tomlinson S, Tritto T, Zhang Z (2007) Constrained analogs of CB-1 antagonists: 1,5,6,7-Tetrahydro-4H-pyrrolo[3,2-c]pyridine-4-one derivatives. *Bioorg Med Chem Lett* 17(3):673–678. doi:10.1016/j.bmcl.2006.10.095
 21. Lange JH, Kruse CG (2008) Cannabinoid CB1 receptor antagonists in therapeutic and structural perspectives. *Chem Rec* 8(3):156–168. doi:10.1002/tcr.20147
 22. Griffith DA, Hadcock JR, Black SC, Iredale PA, Carpino PA, DaSilva-Jardine P, Day R, DiBriano J, Dow RL, Landis MS, O'Connor RE, Scott DO (2009) Discovery of 1-[9-(4-chlorophenyl)-8-(2-chlorophenyl)-9H-purin-6-yl]-4-ethylaminopiperidine-4-carboxylic acid amide hydrochloride (CP-945,598), a novel, potent, and selective cannabinoid type 1 receptor antagonist. *J Med Chem* 52(2):234–237. doi:10.1021/jm8012932 10.1021/jm8012932
 23. Dow RL, Carpino PA, Hadcock JR, Black SC, Iredale PA, DaSilva-Jardine P, Schneider SR, Paight ES, Griffith DA, Scott DO, O'Connor RE, Nduaka CI (2009) Discovery of 2-(2-chlorophenyl)-3-(4-chlorophenyl)-7-(2,2-difluoropropyl)-6,7-dihydro-2H-pyrazolo[3,4-f][1,4]oxazepin-8(5H)-one (PF-514273), a novel, bicyclic lactam-based cannabinoid-1 receptor antagonist for the treatment of obesity. *J Med Chem* 52(9):2652–2655. doi:10.1021/jm900255t
 24. Hurst DP, Lynch DL, Barnett-Norris J, Hyatt SM, Seltzman HH, Zhong M, Song ZH, Nie JJ, Lewis D, Reggio PH (2002) N-(Piperidin-1-yl)-5-(4-chlorophenyl)-1-(2,4-dichlorophenyl)-4-methyl-1H-pyrazole-3-carboxamide (SR141716A) interaction with LYS 3.28 (192) is crucial for its inverse agonism at the cannabinoid CB1 receptor. *Mol Pharmacol* 62(6):1274–1287
 25. Hurst D, Umejiego U, Lynch D, Seltzman H, Hyatt S, Roche M, McAllister S, Fleischer D, Kapur A, Abood M, Shi SP, Jones J, Lewis D, Reggio P (2006) Biarylpyrazole inverse agonists at the cannabinoid CB1 receptor: Importance of the C-3 carboxamide oxygen/lysine3.28(192) interaction. *J Med Chem* 49(20):5969–5987. doi:10.1021/Jm060446b
 26. Shire D, Calandra B, Delpesch M, Dumont X, Kaghad M, Le Fur G, Caput D, Ferrara P (1996) Structural features of the central cannabinoid CB1 receptor involved in the binding of the specific CB1 antagonist SR 141716A. *J Biol Chem* 271(12):6941–6946
 27. Trillou CR, Arnone M, Delgorge C, Gonalons N, Keane P, Maffrand JP, Soubrie P (2003) Anti-obesity effect of SR141716, a CB1 receptor antagonist, in diet-induced obese mice. *Am J Physiol Regul Integr Comp Physiol* 284(2):R345–R353. doi:10.1152/ajpregu.00545.2002
 28. Hagemann WK (2008) The discovery of taranabant, a selective cannabinoid-1 receptor inverse agonist for the treatment of obesity. *Archiv Der Pharmazie* 341(7):405–411. doi:10.1002/ardp.200700255
 29. Shim JY, Welsh WJ, Cartier E, Edwards JL, Howlett AC (2002) Molecular interaction of the antagonist N-(piperidin-1-yl)-5-(4-chlorophenyl)-1-(2,4-dichlorophenyl)-4-methyl-1H-pyrazole-3-carboxamide with the CB1 cannabinoid receptor. *J Med Chem* 45(7):1447–1459
 30. Tong WD, Hong HX, Xie Q, Shi LM, Fang H, Perkins R (2005) Assessing QSAR Limitations - A Regulatory Perspective. *Curr Comput Aid Drug* 1(2):195–205
 31. Carlsson J, Coleman RG, Setola V, Irwin JJ, Fan H, Schlessinger A, Sali A, Roth BL, Shoichet BK (2011) Ligand discovery from a dopamine D(3) receptor homology model and crystal structure. *Nat Chem Biol* 7(11):769–778. doi:10.1038/Nchembio.662
 32. Sun XQ, Li YZ, Li WH, Xu ZJ, Tang Y (2011) Computational investigation of interactions between human H(2) receptor and its

- agonists. *J Mol Graph Model* 29(5):693–701. doi:10.1016/j.jm gm.2010.12.001
33. Cheng FX, Xu ZJ, Liu GX, Tang Y (2010) Insights into binding modes of adenosine A(2B) antagonists with ligand-based and receptor-based methods. *European Journal of Medicinal Chemistry* 45(8):3459–3471. doi:10.1016/j.ejmech.2010.04.039
34. Cheng JX, Liu GX, Zhang J, Xu ZJ, Tang Y (2011) Insights into subtype selectivity of opioid agonists by ligand-based and structure-based methods. *J Mol Model* 17(3):477–493. doi:10.1007/s00894-010-0745-1
35. Lu C, Jin F, Li C, Li W, Liu G, Tang Y (2011) Insights into binding modes of 5-HT_{2c} receptor antagonists with ligand-based and receptor-based methods. *J Mol Model* 17(10):2513–2523. doi:10.1007/s00894-010-0936-9
36. Jin F, Lu C, Sun X, Li W, Liu G, Tang Y (2011) Insights into the binding modes of human beta-adrenergic receptor agonists with ligand-based and receptor-based methods. *Mol Divers* 15(4):817–831. doi:10.1007/s11030-011-9311-8
37. Cherezov V, Rosenbaum DM, Hanson MA, Rasmussen SG, Thian FS, Kobilka TS, Choi HJ, Kuhn P, Weis WI, Kobilka BK, Stevens RC (2007) High-resolution crystal structure of an engineered human beta₂-adrenergic G protein-coupled receptor. *Science* 318(5854):1258–1265. doi:10.1126/science.1150577
38. Shim JY, Welsh WJ, Howlett AC (2003) Homology model of the CB₁ cannabinoid receptor: Sites critical for nonclassical cannabinoid agonist interaction. *Biopolymers* 71(2):169–189. doi:10.1002/Bip. 10424
39. Salo OM, Lahtela-Kakkonen M, Gynther J, Jarvinen T, Poso A (2004) Development of a 3D model for the human cannabinoid CB₁ receptor. *J Med Chem* 47(12):3048–3057. doi:10.1021/jm031052c
40. Montero C, Campillo NE, Goya P, Paez JA (2005) Homology models of the cannabinoid CB₁ and CB₂ receptors. A docking analysis study. *Eur J Med Chem* 40(1):75–83. doi:10.1016/j.ejmech.2004.10.002
41. Lin LS, Ha S, Ball RG, Tsou NN, Castonguay LA, Doss GA, Fong TM, Shen CP, Xiao JC, Goulet MT, Hagmann WK (2008) Conformational analysis and receptor docking of N-[(1S,2S)-3-(4-Chlorophenyl)-2-(3-cyanophenyl)-1-methylpropyl]-2-methyl-2-[[5-(trifluoromethyl)pyridin-2-yl]oxy]propanamide (taranabant, MK-0364), a novel, acyclic cannabinoid-1 receptor inverse agonist. *J Med Chem* 51(7):2108–2114. doi:10.1021/Jm7014974
42. Okada T, Sugihara M, Bondar AN, Elstner M, Entel P, Buss V (2004) The retinal conformation and its environment in rhodopsin in light of a new 2.2 Å crystal structure. *J Mol Biol* 342(2):571–583. doi:10.1016/j.jmb.2004.07.044
43. Shim JY (2009) Transmembrane Helical Domain of the Cannabinoid CB₁ Receptor. *Biophys J* 96(8):3251–3262. doi:10.1016/j.bpj.2008.12.3934
44. Zhang Y, Burgess JP, Brackeen M, Gilliam A, Mascarella SW, Page K, Seltzman HH, Thomas BF (2008) Conformationally constrained analogues of N-(piperidinyl)-5-(4-chlorophenyl)-1-(2,4-dichlorophenyl)-4-methyl-1H-pyrazole-3-carboxamide (SR141716): design, synthesis, computational analysis, and biological evaluations. *J Med Chem* 51(12):3526–3539. doi:10.1021/jm8000778
45. Catalyst User Guide, version 4.10 (Software Package), Accelrys, Inc, San Diego, CA, USA, 2005. <http://accelrys.com/>
46. Accelrys Software Inc., Discovery Studio Modeling Environment, Release 2.1, Accelrys, Inc, San Diego, CA, USA, 2004, <http://accelrys.com/>
47. Fang J, Shen J, Cheng FX, Xu ZJ, Liu GX, Tang Y (2011) Computational Insights into Ligand Selectivity of Estrogen Receptors from Pharmacophore Modeling. *Mol Inform* 30(6–7):539–549. doi:10.1002/minf.201000170
48. Boeckmann B, Bairoch A, Apweiler R, Blatter MC, Estreicher A, Gasteiger E, Martin MJ, Michoud K, O'Donovan C, Phan I, Pilbout S, Schneider M (2003) The SWISS-PROT protein knowledgebase and its supplement TrEMBL in 2003. *Nucleic Acids Res* 31(1):365–370
49. Berman HM, Westbrook J, Feng Z, Gilliland G, Bhat TN, Weissig H, Shindyalov IN, Bourne PE (2000) The Protein Data Bank. *Nucleic Acids Res* 28(1):235–242
50. Schrödinger LLC (2008) Maestro, version 8.5, Schrödinger, LLC, New York, NY
51. Gross M (2011) Anarchy in the proteome. *Chemistry World*, Aug 2011, www.chemistryworld.org
52. Schrödinger LLC (2008) MacroModel, version 9.6, Schrödinger, LLC, New York, NY
53. Morris AL, MacArthur MW, Hutchinson EG, Thornton JM (1992) Stereochemical quality of protein structure coordinates. *Proteins* 12(4):345–364. doi:10.1002/prot.340120407
54. Schrödinger LLC (2005) LigPrep version 2.2, Schrödinger, LLC, New York, NY
55. Schrödinger LLC (2008) Glide version 5.0, Schrödinger, LLC, New York, NY
56. Wears RL, Lewis RJ (1999) Statistical models and Occam's razor. *Acad Emerg Med* 6(2):93–94
57. Kirchmair J, Markt P, Distinto S, Wolber G, Langer T (2008) Evaluation of the performance of 3D virtual screening protocols: RMSD comparisons, enrichment assessments, and decoy selection - What can we learn from earlier mistakes? *J Comput Aided Mol Des* 22:213–228
58. Jain AN, Nicholls A (2008) Recommendations for evaluation of computational methods. *J Comput Aided Mol Des* 22:133–139
59. Telvekar VN, Patel KN (2011) Pharmacophore development and docking studies of the hiv-1 integrase inhibitors derived from N-methylpyrimidones, Dihydroxypyrimidines, and bicyclic pyrimidones. *Chem Biol Drug Des* 78(1):150–160. doi:10.1111/j.1747-0285.2011.01130.x
60. Weber KC, de Lima EF, de Mello PH, da Silva ABF, Honorio KM (2010) Insights into the Molecular Requirements for the Anti-obesity Activity of a Series of CB₁ Ligands. *Chem Biol Drug Des* 76(4):320–329. doi:10.1111/j.1747-0285.2010.01016.x
61. Baldwin JM, Schertler GF, Unger VM (1997) An alpha-carbon template for the transmembrane helices in the rhodopsin family of G-protein-coupled receptors. *J Mol Biol* 272(1):144–164. doi:10.1006/jmbi.1997.1240
62. McAllister SD, Rizvi G, Anavi-Goffer S, Hurst DP, Barnett-Norris J, Lynch DL, Reggio PH, Aboud ME (2003) An aromatic microdomain at the cannabinoid CB₁ receptor constitutes an agonist/inverse agonist binding region. *J Med Chem* 46(24):5139–5152. doi:10.1021/Jm0302647
63. Kim KH, Kim ND, Seong BL (2010) Pharmacophore-based virtual screening: a review of recent applications. *Expert Opin Drug Dis* 5(3):205–222. doi:10.1517/17460441003592072